frontiers | Frontiers in Energy Research

TYPE Original Research
PUBLISHED 31 January 2023
DOI 10.3389/fenrg.2022.1021189

OPEN ACCESS

EDITED BY
Biyun Chen,
Guangxi University, China

REVIEWED BY
Muhammad Faizan Tahir,
South China University of Technology, China
Inung Wijayanto,
Telkom University, Indonesia

*CORRESPONDENCE
Jiangbo Shen,
446594701@qq.com

SPECIALTY SECTION
This article was submitted to Smart Grids,
a section of the journal
Frontiers in Energy Research

RECEIVED 17 August 2022
ACCEPTED 31 October 2022
PUBLISHED 31 January 2023

CITATION
Shen J, Huang S, Liu C, Li S and Wu J (2023), Optimal configuration method of wind farm hybrid energy storage based on EEMD-EMD and grey relational degree analysis.
Front. Energy Res. 10:1021189.
doi: 10.3389/fenrg.2022.1021189

Optimal configuration method of wind farm hybrid energy storage based on EEMD-EMD and grey relational degree analysis

Jiangbo Shen[1,2]*, Sujuan Huang[2], Chunjing Liu[1], Shaodong Li[3] and Jinwen Wu[2]

[1]School of Electrical and Electronic Engineering, Anhui Institute of Information Engineering, Wuhu, China, [2]Pujiang College, Nanjing University of Technology, Nanjing, China, [3]Guangxi Electric Power Vocational and Technical College, Nanning, China

The large-scale grid connection of new energy wind power generation has caused serious challenges to the power quality of the power system. The hybrid energy storage system (HESS) is an effective means to smooth the fluctuation of wind power and improve the economy of the system. In order to determine the optimal capacity configuration of the hybrid energy storage system, first, a decomposition method which combines ensemble empirical mode decomposition (EEMD) and empirical mode decomposition (EMD) is proposed, and a series of intrinsic mode functions are obtained, the grey correlation analysis method is used to analyze the similarity, and the components with similar correlation values are reconstructed to obtain high-frequency and low-frequency components; second, considering the battery life loss of the hybrid energy storage system, with the goal of minimizing the entire life cycle cost, the optimal configuration model of hybrid energy storage capacity is established, and different energy storage schemes are analyzed to obtain the energy storage configuration scheme with the best economy; finally, based on the typical daily historical data of a wind farm, the effectiveness and economy of the proposed method are verified.

KEYWORDS

hybrid energy storage system, ensemble empirical mode decomposition, grey relational analysis, life cycle cost, optimal configuration of energy storage

1 Introduction

In the renewable energy power generation system, wind power generation and photovoltaic power generation have the advantages of economy, environmental protection, and cleanliness and will become the main body of new energy power generation in the future (Sun et al., 2019). Since wind power generation is characterized by intermittency, volatility, and uncertainty, the safe and stable operation of the power system will be greatly challenged by large-scale wind power grid connection (Samiet al., 2018; Tabart et al., 2017). The configuration of energy storage at the wind farm can smooth the output fluctuation of wind power, reduce the influence of

wind power grid-connected system on the power system (Lou et al., 2014), significantly improve the power quality of the system, and greatly improve the economic benefits of wind power (Han et al., 2017). With the improvement in the economic benefits of the combined wind storage system and the promotion of the economic value of the energy storage system to smooth wind power fluctuations, it is necessary to study the capacity optimization of energy storage at wind farms (Gan et al., 2019).

Due to good complementarity, the hybrid energy storage system can smooth the wind power fluctuation and better guarantee the stability and economy of wind power grid-connected system compared with the single energy storage system (He et al., 2020). There are mainly two types of energy storage media: one is energy-based energy storage and the other is power-based energy storage, and the combination of the two can achieve complementary advantages (Mamun et al., 2018). Battery energy storage belongs to energy-based energy storage, supercapacitor belongs to power-based energy storage, and combining the two forms a hybrid energy storage type, which is used to not only improve the output characteristics of the energy storage system but also greatly reduce the output frequency of the battery energy storage, prolong its service life, and give full play to the advantage of hybrid energy storage, thus making up for the inherent defect in a single energy storage system. However, at the current technology level, the cost of the energy storage system is still high in capacity configuration. On the premise of meeting the requirements of wind power fluctuation suppression, the capacity of the hybrid energy storage system and the ratio of internal energy storage components in the system are the key issues to be solved when hybrid energy storage technology is applied to practical projects.

The optimal allocation of hybrid energy storage system capacity has been widely and deeply studied by scholars at home and abroad. In Bitaraf et al. (2015), discrete Fourier transform (DFT) and discrete wavelet transform (DWT) are proposed to deal with wind power, but the processing effect is still not ideal due to the non-stationarity of wind power. Guo et al. (2020) use the wavelet packet principle to decompose the hybrid energy storage system, so as to determine the number of decomposition layers of the wavelet packet. The low-frequency and high-frequency components obtained by wavelet packet decomposition can be assigned to batteries and supercapacitors as charge and discharge power commands. Since the number of decomposed layers needs to be determined independently, the results of energy storage optimization configuration are greatly affected. In Yuan et al. (2015) and Han et al. (2014), the empirical mode decomposition method is proposed to decompose the wind active power, but directly using the EMD method will cause problems such as large noise and mode aliasing. Fu et al. (2019) and Guo et al. (2020) use the ensemble empirical mode decomposition method to process the active power of wind farms and design spatiotemporal filters to obtain high-frequency power components and low-frequency power components, respectively. However, due to the instability of wind power signals, the difficulty of order selection of the spatiotemporal filter and the noise of EEMD make the accuracy of the decomposed high–low frequency power signal not high.

The EEMD method is effective for blasting signals, intermittent signals, and other sudden situations, and EMD is effective for eliminating the general signals mentioned previously (Zheng et al., 2013). Through the study of various improved empirical mode decomposition methods, almost all the improved empirical mode decomposition methods have to add EMD processing in the last step of their basic principle formula derivation. Therefore, in order to reduce mode confusion, in the first stage of this paper, EEMD is used to deal with the original wind power which contains a large number of gap signals and random signals; in order to ensure the completeness and orthogonality of signals, mixed energy storage power is processed by EMD in the second stage, which can allocate high- and low-frequency power reasonably and further improve the economy of the system.

The life loss of batteries and supercapacitors always exists in engineering application because the service life of supercapacitors is long and can operate stably in the planning cycle. Generally, in the capacity configuration, the service life can be set to a fixed value according to practical experience. Due to the limited cycle life of the lithium battery, frequent charge and discharge and high rate charge and discharge will sharply reduce its service life, increase the number of replacements in the whole life cycle, and affect the economy of the hybrid energy storage system. Therefore, the impact of battery life loss is mainly considered (Hemmati et al., 2017). In Han et al. (2018), a hybrid energy storage system is constructed using the battery and supercapacitor, and the battery discharge depth is calculated using the rain-flow counting method to obtain the equivalent cycle life of the battery so as to establish a hybrid energy storage capacity configuration model. Li et al. (2018) show that whether the battery life loss considered in the planning period will affect the investment returns of energy storage when calculating the economy, resulting in a misjudgment of the economy of the integrated energy system. Guo et al. (2021) analyze the relationship between the complementary characteristics of the hybrid energy storage system and battery life loss and conclude that the hybrid energy storage configuration result of the comprehensive energy system in the park is affected by battery life loss, and the complementary characteristics can effectively delay battery decay.

The determination of boundary frequency is related to the economy of system capacity allocation and also affects the effect of the hybrid energy storage system on wind power fluctuation suppression. Zhang et al. (2016) and Ge et al. (2017) propose to use the instantaneous frequency–time curve to find the cutoff frequency, but the more the components of power

decomposition, the more complex the energy aliasing on the curve, which brings difficulties to find the cutoff frequency. Guo et al. (2020) put forward the method of selecting the filtering order successively, aiming at minimizing the annual comprehensive cost, and determining the optimal filtering order by sorting, but the workload is too large. Therefore, it is very important to select the dividing frequency point to reduce the workload and calculate the accuracy.

Therefore, this paper comprehensively considers the problems existing in the aforementioned literature studies and proposes a wind farm hybrid energy storage system capacity optimal allocation model based on the combined application of modal decomposition method of EEMD and EMD and gray relational degree analysis. First, the output power signal of the wind farm is decomposed by EEMD to obtain the target grid-connected power and hybrid energy storage power that meet the grid-connected requirements. Second, hybrid energy storage power using the EMD method is decomposed into different frequency bands of the subcomponent, and grey correlation analysis method is used to determine these subcomponent division frequency points, classifying a component into high-frequency power signal and low-frequency power signal, with the high-frequency signal as the reference power of the power-based energy storage type and low-frequency signal as the reference power of the energy-based energy storage type. A mathematical model of HESS life cycle cost (LCC) is constructed. In order to improve the economic and operational benefits and to smooth the wind power fluctuation in real time, an optimal allocation method of HESS power and capacity is proposed with the goal of minimizing LCC. Finally, the model and method proposed in this paper are used to analyze the real data of a wind farm.

2 Raw wind power allocation based on ensemble empirical mode decomposition

2.1 Ensemble empirical mode decomposition

Due to the nonlinear and non-stationarity characteristics of wind power output signals, the traditional frequency-domain method for decomposition wind power signals is prone to modal aliasing, while the EEMD method can solve the modal aliasing problem. The principle of EEMD is described in the literature.

The process of decomposition of the original wind power signal by the EEMD method is as follows:

(1) The white Gaussian noise signal $\omega(t)$ is added to the original power signal $P_W(t)$ to obtain a common signal, i.e.,

$$P(t) = P_W(t) + \omega(t), \tag{1}$$

$$P(t) = r_n(t) + \sum_{i=1}^{n} c_i(t), \tag{2}$$

(2) Through EMD decomposition of the signal $P(t)$, the intrinsic mode function (IMF) component is

where $r_n(t)$ is the afterwave signal and $c_i(t)$ is the IMF component of the natural mode function of the i (i = 1,2, . . . ,n) layer, whose distribution order is from high to low frequency.

(3) The white Gaussian noise signal is added to the original power signal $P_W(t)$ for the j time, and Step 1 and Step 2 are repeated to calculate acquirability:

$$\begin{cases} P_j(t) = P_W(t) + \omega_j(t), \\ P_j(t) = r_{jn}(t) + \sum_{i=1}^{n} c_{ji}(t), \end{cases} \tag{3}$$

where $c_{ji}(t)$ is the ith IMF component (3) obtained by EMD after white Gaussian noise is added for the jth time.

(4) When $c_{ji}(t)$ is averaged, the power signal value of the ith IMF component is

$$c_i(t) = \frac{1}{N}\sum_{j=1}^{N} c_{ji}(t), \tag{4}$$

where N is the overall average times of adding the Gaussian white noise signal.

$$P_W(t) = r_n(t) + \sum_{i=1}^{n} c_i(t). \tag{5}$$

(5) The reconstructed signal $P_W(t)$ obtained after EEMD is

2.2 Adaptive ensemble empirical mode decomposition of wind power

According to the EEMD method, the wind power signal is decomposed into a series of IMF components and a residual component according to the frequency distribution order. The spatiotemporal filter is designed to obtain the grid-connected power which is smooth and meets the requirements of the national grid connection standard. The structure diagram of the wind storage power generation system is shown in Figure 1.

The low-frequency part (grid-connected power) is given as follows:

$$P_g(t) = r_n(t) + \sum_{i=k}^{n} c_i(t). \tag{6}$$

$$P_{HESS}(t) = \sum_{i=1}^{k-1} c_i(t), \tag{7}$$

The high-frequency part (power of the hybrid energy storage system) is given as follows:where $P_g(t)$ is grid-connected power,

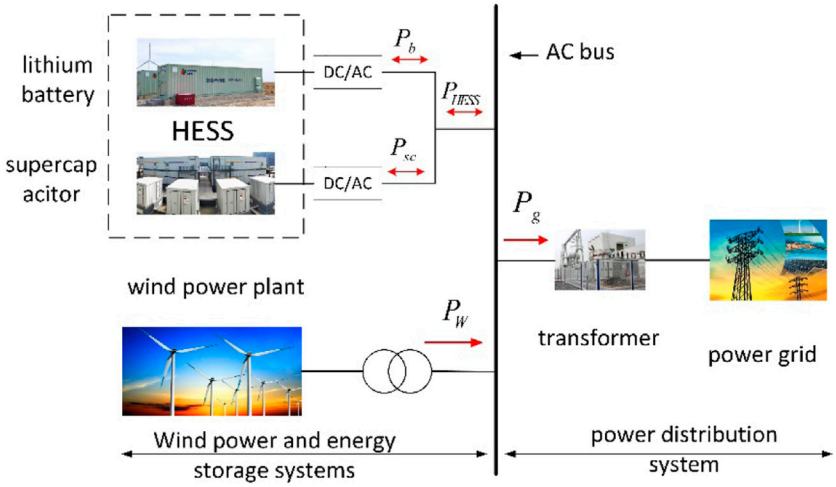

FIGURE 1
Structure diagram of the wind storage power generation system.

$P_{\mathrm{HESS}}(t)$ is hybrid energy storage power, and k is the filtering order of the spatiotemporal filter.

At time t, the maximum power volatility of wind power output in 1 min or 10 min can be calculated according to Eqs 8, 9.

$$\delta_{1\,\mathrm{min}.Pg} = \frac{\max\limits_{\Delta t=1,2,\cdots,59} P_{\mathrm{g}}(t) - \min\limits_{\Delta t=1,2,\cdots,59} P_{\mathrm{g}}(t)}{P_o}, \tag{8}$$

$$\delta_{10\,\mathrm{min}.Pg} = \frac{\max\limits_{\Delta t=1,2,\cdots,599} P_{\mathrm{g}}(t) - \min\limits_{\Delta t=1,2,\cdots,599} P_{\mathrm{g}}(t)}{P_o}, \tag{9}$$

where P_{o} is the installed capacity of the wind farm, and the 1 min/10 min volatility of the grid-connected power of wind power should meet the national standards for wind power grid-connected at any time. In this paper, the installed capacity of the 50-MW wind farm is selected, and its volatility requirement is given as follows:

$$\begin{cases} \delta_{1\,\mathrm{min}.Pg} \leqslant \dfrac{1}{10}, \\ \delta_{10\,\mathrm{min}.Pg} \leqslant \dfrac{1}{3}. \end{cases} \tag{10}$$

First, judge whether the original output power $P_{\mathrm{W}}(t)$ of wind power meets the standard of wind power grid-connected volatility. If $P_{\mathrm{W}}(t)$ meets the standard, it can be directly connected to the grid. If the standard is not met, the EEMD method is used to decompose $P_{\mathrm{W}}(t)$, with $n = k$ and the value of k increasing in cycles, and $P_{\mathrm{g}}(t)$ is judged according to Eq. 10. When the volatility exceeds the grid-connected standard for the first time, the filtering order $k = k + 1$ can be determined as the optimal value, and then the adaptive decomposition of wind power is completed.

3 Active power distribution of hybrid energy storage based on the empirical mode decomposition method

3.1 Active power decomposition of hybrid energy storage by empirical mode decomposition

Empirical mode decomposition (EMD) is an adaptive time–frequency processing method for non-stationary and nonlinear signals. The empirical mode decomposition method in the case of no pre-determined basis function can use its time scale characteristics of the signal processing, the essence of which is to process signal into frequency from high to low in a series of intrinsic mode functions, after EMD being a child of the modal number far less than a child of the modal number wavelet algorithm and has good practicability. The hybrid energy storage power of HESS is decomposed by EMD to obtain a series of natural mode functions of frequency distribution. By choosing the dividing frequency, the aforementioned decomposed signals are reconstructed into high-frequency components and low-frequency components. The high-frequency component is used as the reference power of power-based energy storage, while the low-frequency component is used as the reference power of energy-based energy storage, i.e.,

$$P_{\mathrm{HESS}}(t) = P_{\mathrm{w}}(t) - P_{\mathrm{g}}(t), \tag{11}$$

$$P_{\mathrm{HESS}}(t) = P_b(t) + P_{sc}(t), \tag{12}$$

$$P_{\mathrm{HESS}}(t) = \sum_{i=1}^{n} P_i(t) + P_r(t), \tag{13}$$

$$\begin{cases} P_{\mathrm{sc}}(t) = P_{\mathrm{high}}(t) = \sum_{i=1}^{j} P_i(t), \\ P_{\mathrm{b}}(t) = P_{\mathrm{low}}(t) = \sum_{i=j+1}^{n} P_i(t) + P_r(t), \end{cases} \quad j \in \{1, 2, \cdots, n\}, \tag{14}$$

where $P_{\mathrm{HESS}}(t)$ is the power of hybrid energy storage, $P_{\mathrm{b}}(t)$ is the power of the lithium battery, and $P_{\mathrm{sc}}(t)$ is the power of the supercapacitor. $P_{\mathrm{i}}(t)$ is the IMF components of each order processed by the EMD method, i = 1,2,⋯,n. $P_{\mathrm{r}}(t)$ is the aftereffect component. $P_{\mathrm{high}}(t)$ is the high-frequency component, which is used as the reference power of supercapacitor energy storage. $P_{\mathrm{low}}(t)$ represents the low-frequency component which is used as the reference power of lithium battery energy storage.

3.2 Active power reconstruction of the hybrid energy storage system based on grey correlation analysis

The grey relational analysis method has the advantage of clearly showing the power signal of the hybrid energy storage system with nonlinear and non-stationary characteristics, which are not only simple to calculate but also widely applied in engineering (Zheng et al., 2021). The EMD hybrid energy storage system uses a list of each order power signal output power components and the aftermath of the IMF. Grey correlation analysis was used to determine the IMF components, and aftermath similarity analysis was used to determine the correlation values and similar correlation degrees were segregated for reconstructing them into high-frequency and low-frequency parts. The supercapacitor was used to smooth the output of the high-frequency part, and the smoothening of the output of the low-frequency part was carried out by the lithium battery. The specific steps of grey correlation analysis are as follows (Wang et al., 2017; Lin et al., 2021):

(1) Determine the comparison sequence

An analysis matrix consisting of IMF components and aftereffect components after EMD is constructed.

$$P = \begin{bmatrix} p_{11} & p_{12} & \cdots & p_{1n} \\ p_{21} & p_{22} & \cdots & p_{2n} \\ \vdots & \vdots & & \vdots \\ p_{m1} & p_{m2} & \cdots & p_{\mathrm{mn}} \end{bmatrix}. \tag{15}$$

(2) Normalize the comparison sequence, also known as dimensionless processing. In this paper, Eq. 16 is used to normalize the IMF component and the afterwave component of each order power signal, respectively, so that they can be transformed into data at an interval of (0,1). Then, the dimensionless processing formula is as follows:

$$p_{\mathrm{ij}}^{B} = \frac{p_{ij} - p_{j\min}}{p_{j\max} - p_{j\min}}, i = 1, 2, \ldots, m; j = 1, 2, \ldots, n. \tag{16}$$

The resulting dimensionless matrix is:

$$P' = \begin{bmatrix} p'_{01} & p'_{02} & \cdots & p'_{0n} \\ p'_{11} & p'_{12} & \cdots & p'_{12} \\ \vdots & \vdots & & \vdots \\ p'_{m1} & p'_{m2} & \cdots & p'_{\mathrm{mn}} \end{bmatrix}. \tag{17}$$

The first behavior is a reference sequence, whose formula is (18). The reference sequence is composed of the maximum value of each column of the comparison sequence. In this sequence, i ($1 \leqslant i \leqslant m$) elements are denoted as $p'_{0i,\mathrm{opt}} = \max\{p'_i\}$ ($1 \leqslant j \leqslant n$), and $p'_{0i,\mathrm{opt}}$ is the maximum of n items.

$$P_0' = \left[p'_{01}, p'_{02}, \ldots, p'_{0n}\right]. \tag{18}$$

(3) Generate difference matrix

Through Eq.19, matrix $Z=(z_{\mathrm{ij}})_{m\times n}$ can be obtained, and the difference matrix is formed according to Eq. 20.

$$z_{\mathrm{ij}} = \left|p'_{0i,\mathrm{opt}} - p'_{ij}\right|, (1 \leqslant j \leqslant n), \tag{19}$$

$$Z = \begin{bmatrix} z_{11} & z_{12} & \cdots & z_{1n} \\ z_{21} & z_{22} & \cdots & z_{2n} \\ \vdots & \vdots & & \vdots \\ z_{m1} & z_{m2} & \cdots & z_{\mathrm{mn}} \end{bmatrix}. \tag{20}$$

(4) Determine the target reference sequence and comparison sequence, and the grey correlation coefficient formula of the reference sequence and comparison sequence is

$$\xi_{\mathrm{ij}} = \frac{\mathrm{minimin}\left(z_{\mathrm{ij}}\right) + \rho\,\mathrm{maxmax}\left(z_{\mathrm{ij}}\right)}{\left(z_{\mathrm{ij}}\right) + \rho\,\mathrm{maxmax}\left(z_{\mathrm{ij}}\right)}, \tag{21}$$

where ξ_{ij} is the correlation coefficient and ρ is the grey discrimination coefficient, usually 0.5; i = 1,2,3 . . . ,m; j = 2,3, . . . ,n.

(5)3510915613918000 Substitute Eq. 21 into the correlation degree formula Eq. 22 to obtain the correlation degree between each comparison sequence and the reference sequence, i.e.,

$$r_i = \frac{1}{n}\sum_{j=1}^{m} \xi_{\mathrm{ij}}, \tag{22}$$

where r_{i} is the correlation degree.

(6) Divide those with similar correlation degrees into two groups and reconstruct them into high-frequency part and low-frequency part, respectively, as shown in Eq. 14.

4 Optimal capacity configuration of hybrid energy storage system resource identification initiative

4.1 Rated power configuration

Assuming that the rated power of the energy-type energy storage lithium battery is P_{rate}, taking into consideration the energy conversion efficiency of the converter and the charge and discharge efficiency of the energy storage device, then

$$P_{rate} = \max\left\{\left|\max_{t\in(t_0,t_0+T)}(P_b(t))\right| \times\left|\eta_{\text{DC-DC}}\eta_{\text{DC-AC}}\eta_c, \frac{\left|\min_{t\in(t_0,t_0+T)}(P_b(t))\right|}{\eta_{\text{DC-DC}}\eta_{\text{DC-AC}}\eta_d}\right\}, \quad (23)$$

where t_0 is the initial moment; $\eta_{\text{DC-AC}}$ and $\eta_{\text{DC-DC}}$ are the conversion efficiencies of two converters, DC-AC and DC-DC, respectively; and η_c and η_d are the charging efficiency and discharge efficiency of the energy storage device, respectively. The calculation method of the power-type energy storage supercapacitor is similar to that of the energy-type energy storage lithium battery.

4.2 Rated capacity configuration

Set the rated capacity of the energy-type lithium energy storage battery as E_{rate} and set the initial state of charge of the energy-type energy storage lithium battery at time 0 as SOC_0, then the state of charge SOC_k at time k is

$$\begin{cases} \text{SOC}_k = SOC_0 + \dfrac{\int_0^{k\Delta T} P_n(t)\mathrm{d}t}{E_{rate}}, \\ \text{SOC}_{\min} \le SOC_k \le SOC_{max}, \end{cases} \quad (24)$$

where ΔT is the output time interval of the energy-type energy storage lithium battery and $P_n(t)$ is the power of energy-type energy storage after considering the conversion efficiency and charge and discharge efficiency, and its formula is

$$P_n(t) = \begin{cases} P_b(t)\eta_{\text{DC-DC}}\eta_{\text{DC-AC}}\eta_c, P_n(t) > 0, \\ \dfrac{P_b(t)}{\eta_{\text{DC-DC}}\eta_{\text{DC-AC}}\eta_d}, P_n(t) \le 0, \end{cases} \quad (25)$$

where T is the research duration, and the rated capacity E_{rate} of the energy-type energy storage lithium battery can be calculated as follows:

$$E_{\text{rate}} \ge \max\left\{\frac{\max_{t\in T}\int_0^{k\Delta T} P_n(t)\mathrm{d}t}{SOC_{\max} - SOC_0}, \frac{-\min_{t\in T}\int_0^{k\Delta T} P_n(t)\mathrm{d}t}{SOC_0 - SOC_{\min}}\right\}. \quad (26)$$

When SOC_0 satisfies Eq. 27 and is equal to Eq. 26, the rated capacity of the energy-type energy storage lithium battery is of the minimum value. The calculation method of the power-type energy storage supercapacitor is similar to that of the energy-type energy storage lithium battery.

$$SOC_0 = \frac{\max_{t\in T}\left[\int_0^{k\Delta T} P_n(t)\mathrm{d}t\right]\text{SOC}_{\min} - \min_{t\in T}\left[\int_0^{k\Delta T} P_n(t)\mathrm{d}t\right]\text{SOC}_{\max}}{\max_{t\in T}\left[\int_0^{k\Delta T} P_n(t)\mathrm{d}t\right] - \min_{t\in T}\left[\int_0^{k\Delta T} P_n(t)\mathrm{d}t\right]}. \quad (27)$$

4.3 Battery life estimation model by the rain-flow counting method

The life of the lithium battery is mainly related to the depth of discharge (DOD) and the number of charges and discharges, which affect the life of the battery. In this paper, the discharge depth and cycle life of the lithium battery in each cycle are calculated by the rain-flow cycle counting method. The mathematical model between cycle life and discharge depth can be expressed by formula (28) (Li et al., 2020; Han et al., 2018).

$$N_{\text{ctf}} = -1302D_{\text{OD}}^5 + 4427D_{\text{OD}}^3 - 8925D_{\text{OD}} + 10500, \quad (28)$$

where D_{OD} is the discharge depth of the lithium battery and N_{ctf} is the cycle life at the corresponding depth.

The rain-flow counting method can be used to obtain n cycles of DOD during the battery working cycle according to the battery SOC curve, denoted as D_{OD} (1)、D_{OD} (2)、…、D_{OD}(n), where N_{m} $(D_{\text{OD}}(i))$ is denoted as the maximum number of charge–discharge cycles corresponding to the ith discharge depth, then the decay rate of battery life can be expressed as

$$\gamma = \sum_{i=1}^{n}\frac{1}{N_{\text{m}}(D_{\text{OD}}(i))} \times 100\%, \quad (29)$$

where γ is the battery decay rate.

If the battery has gone through N working cycles, the remaining battery life can be expressed as

$$R = 1 - \sum_{j=1}^{N}\gamma(j), \quad (30)$$

where R is the remaining battery life. When $R = 0$, the battery life reaches its limit.

$$T_{\text{b}} = \frac{1}{365\gamma\lambda}, \quad (31)$$

where T_{b} is the service life of the energy storage lithium battery (unit: year a) and λ is the annual utilization rate of the energy storage lithium battery.

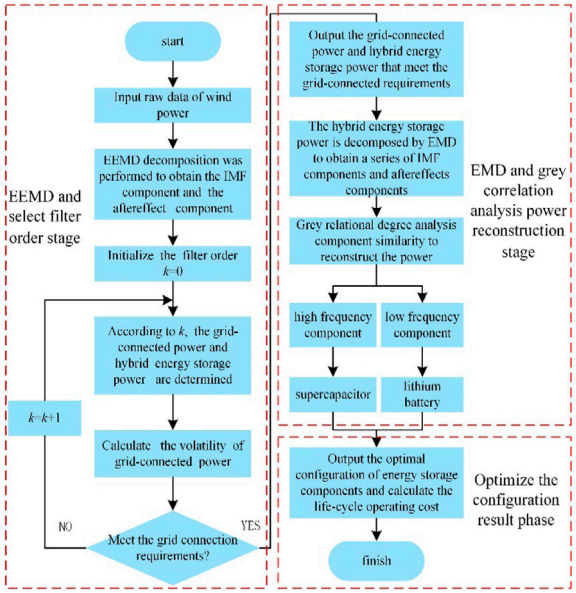

FIGURE 2
Flow chart of hybrid energy storage capacity optimization configuration algorithm.

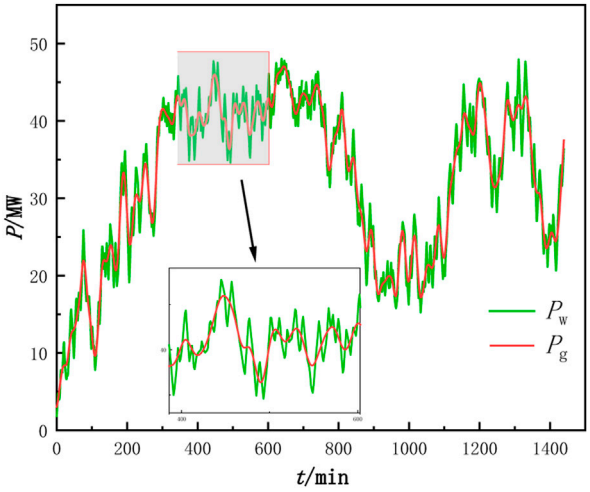

FIGURE 3
Raw wind power and grid-connected power.

4.4 Economic model of the hybrid energy storage system

The theory meaning of whole life cycle cost C_{LCC} is produced in the whole life cycle period of the sum of all direct or indirect costs, including the hybrid energy storage system life cycle for T years, the discount rate for i, and hybrid energy storage component replacement for n times. The target is a hybrid energy storage system for the minimum whole life cycle cost, and the full life cycle cost model is determined as follows:

$$\min C_{LCC} = C_{\text{inv}} + C_{\text{rep}} + C_{\text{om}} + C_{\text{scr}} - C_{\text{res}}, \tag{32}$$

$$C_{inv} = C_{pinv}P_{rate} + C_{einv}E_{rate}, \tag{33}$$

$$C_{\text{rep}} = \sum_{k=1}^{n}\left(C_{\text{prep}}P_{\text{rate}} + C_{\text{erep}}E_{\text{rate}}\right)\left[\frac{P}{F,i}\left(\frac{kT}{n+1}\right)\right], \tag{34}$$

$$C_{\text{om}} = C_{\text{pom}}P_{\text{rate}}\left(P/A,i,T\right) + \sum_{t=1}^{T}C_{\text{eom}}Q_{\text{ess}}\left(t\right)\left(\frac{P}{F,i,T}\right), \tag{35}$$

$$C_{\text{scr}} = \left(C_{\text{pscr}}P_{\text{rate}} + C_{\text{escr}}E_{\text{rate}}\right)\left(n+1\right)\left(\frac{P}{F,i,T}\right), \tag{36}$$

$$C_{\text{res}} = \sigma_{\text{res}}\left(C_{\text{inv}} + C_{\text{rep}}\right)\left(\frac{P}{F,i,T}\right), \tag{37}$$

where C_{inv}, C_{rep}, C_{om}, C_{scr}, and C_{res} are the initial investment cost, regular replacement cost, operation and maintenance cost, waste treatment cost, and recovery and utilization residual value of the hybrid energy storage system, respectively; C_{pinv}, C_{einv}, C_{prep}, C_{erep}, C_{pom}, C_{eom}, C_{pscr}, and C_{escr} represent the unit initial investment power coefficient, unit initial investment capacity coefficient, unit periodic replacement power coefficient, unit periodic replacement capacity coefficient, unit operations and maintenance power coefficient, unit operations and maintenance capacity coefficient, unit waste-processing power coefficient, and unit waste-processing capacity coefficient, respectively; P_{rate} and E_{rate} are rated power and rated capacity of the energy storage element, respectively; $(P/F,i,t)=(1+i)^{-t}$; $Q_{\text{ess}}(t)$ is the annual charge and discharge amount; σ_{res} is the recovery salvage value rate, which is 3%–5%; n = ceil $(T/T_x\text{-}1)$, $x = b$ or $x = sc$; the function ceil(z) is the smallest integer at least z; $(P/A,i,T) = \frac{(1+i)^{T}-1}{i(1+i)^{T}}$.

5 Algorithm flow

The detailed flow chart of the algorithm used in this paper is shown in Figure 2. This process is mainly composed of three stages: EEMD and filtering order selection stage, EMD and grey relational degree analysis power reconstruction stage, and optimization configuration result stage.

Step 1: Since the EEMD decomposition method has strong adaptability for nonlinear or non-stationary signal processing, the original wind power $P_{\text{W}}(t)$ is decomposed by EEMD.

Step 2: The wind power signal is decomposed by EEMD into a finite number of IMF components with different frequency broadband and a residual component. By determining the order k of the spatiotemporal filter, the smooth grid-connected power $P_{\text{g}}(t)$ and the high-frequency partial power $P_{\text{HESS}}(t)$ for hybrid energy storage suppression can be obtained.

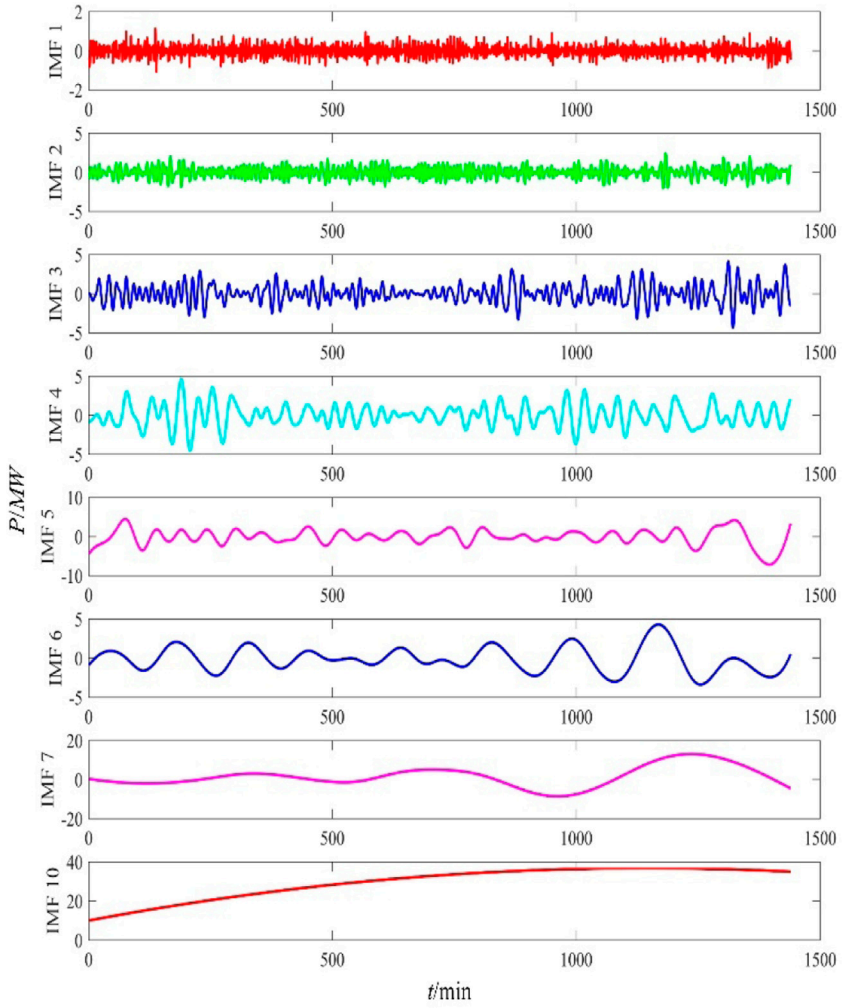

FIGURE 4
Decomposition of raw wind power by EEMD.

Step 3: Determine whether the obtained power meets the requirements of grid-connected by the maximum power fluctuation of 1 min or 10 min. The grid-connected power smoothing effect is closely related to the selection of the *k*-value. When the *k*-value increases, the wind power smoothing effect will be better, but the capacity of the hybrid energy storage system will increase. On the contrary, the standard for wind power grid connection will not be met.

Step 4: The decomposition of EEMD requires a large amount of calculation, and the decomposition will have many false components and other defects, while the reconstruction error of EMD is small. Therefore, the decomposition of hybrid energy storage power by EMD can achieve the purpose of reasonable power distribution.

Step 5: hybrid energy storage power by the EMD, to get a list of each order power signal components and the aftermath of the IMF, degrees of the grey relation analysis method were used to determine the IMF components and aftermath similarity analysis was used to determine the correlation values and similar correlation degrees were segregated for reconstructing them into high-frequency and low-frequency parts. The supercapacitor was used to smooth the output of the high-frequency part, and the low-frequency part was smoothed by the lithium battery.

Step 6: Obtain the hybrid energy storage power configuration and capacity configuration scheme, and calculate the system life cycle operation cost.

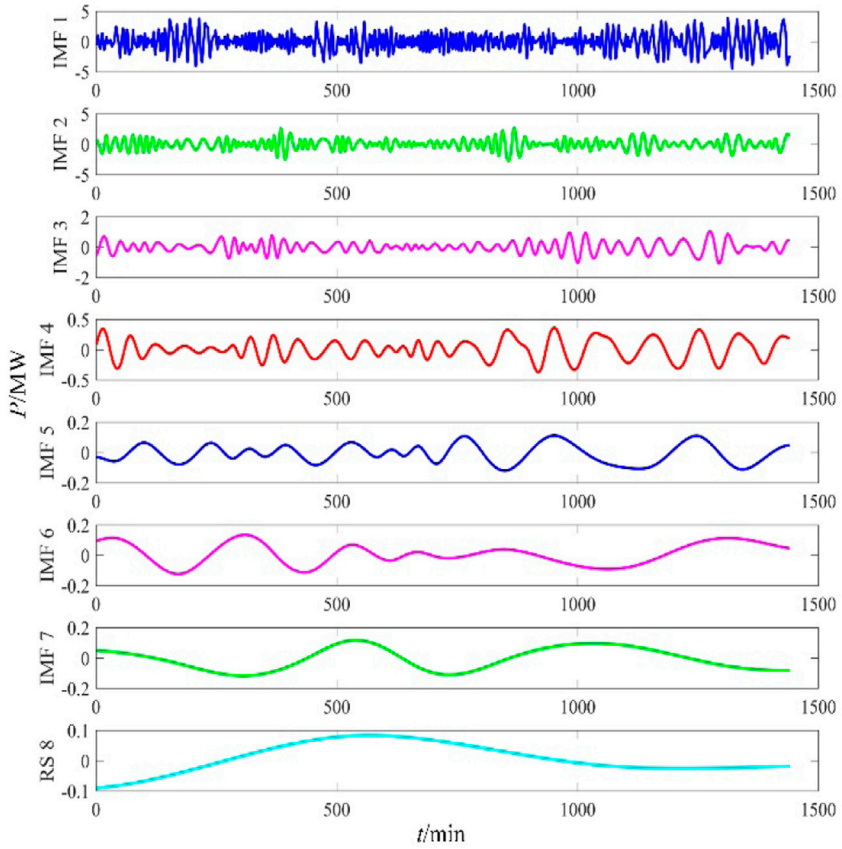

FIGURE 5
EMD decomposition hybrid energy storage power.

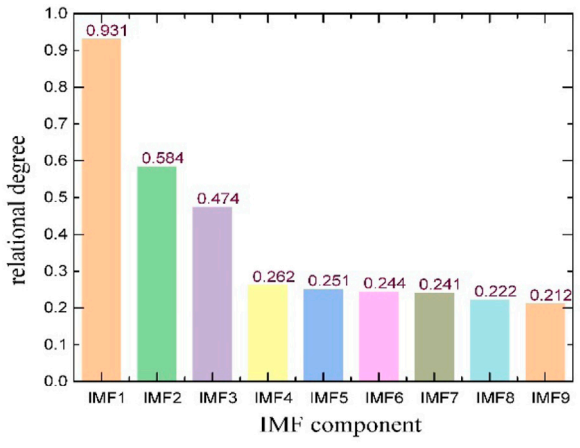

FIGURE 6
Grey correlation analysis of each component.

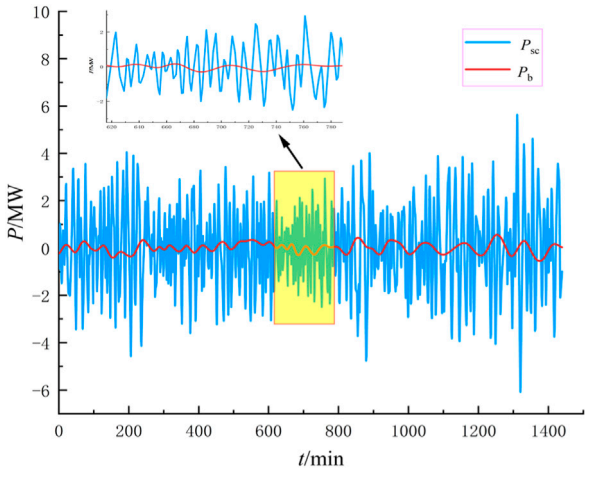

FIGURE 7
Power instruction of hybrid energy storage after reconstruction.

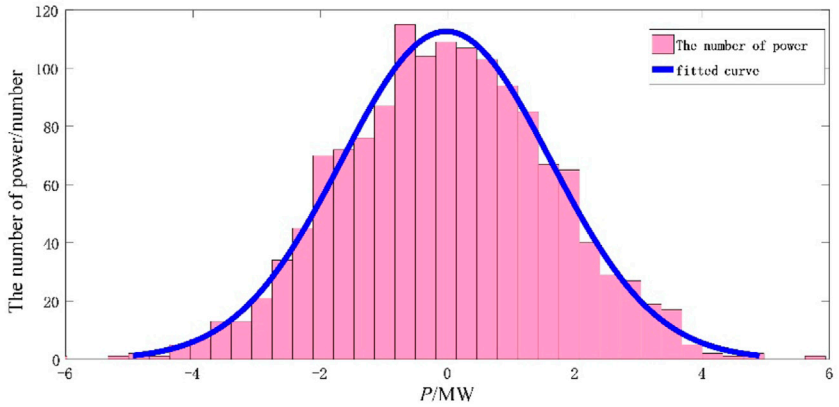

FIGURE 8
Power distribution diagram of the supercapacitor.

TABLE 1 Capacity configuration results of HESS.

Configuration method	Configuration result	Single energy storage scheme	Hybrid energy storage scheme	
		Scheme 1	Scheme 2	
		Lithium battery	Lithium battery	Super capacitor
EMD	Rated power/MW	19.10	13.83	9.93
	Rated capacity/(MW·h)	1.03	0.72	0.40
	Cost/¥	4.30 × 108	3.81 × 108	
EEMD	Rated power/MW	7.37	4.98	3.30
	Rated capacity/(MW·h)	0.41	0.29	0.13
	Cost/¥	2.58 × 108	2.09 × 108	
Methods in this paper	Rated power/MW	7.27	0.67	7.08
	Rated capacity/(MW·h)	0.40	0.04	0.28
	Cost/¥	2.56 × 108	7.63 × 107	

6 Analysis of examples

In this paper, a wind farm with 50 MW installed capacity is taken as an example (Ding et al., 2019). Its typical daily wind power curve and grid-connected power curve after adaptive EEMD are shown in Figure 3, with a sampling interval of 1 min. The *SOC* upper and lower limits are 0.1–0.9, and the charge and discharge efficiency is 0.90.

6.1 Determining the order of the spatiotemporal filter

The original wind power signal was decomposed by EEMD, and nine layers of IMF components with different frequency bands and one layer of aftereffect component were obtained, respectively. IMF components are, respectively, expressed as IMF1–IMF9, where IMF1 is the highest frequency part, IMF9 is the lowest frequency part, and the afterwave part is

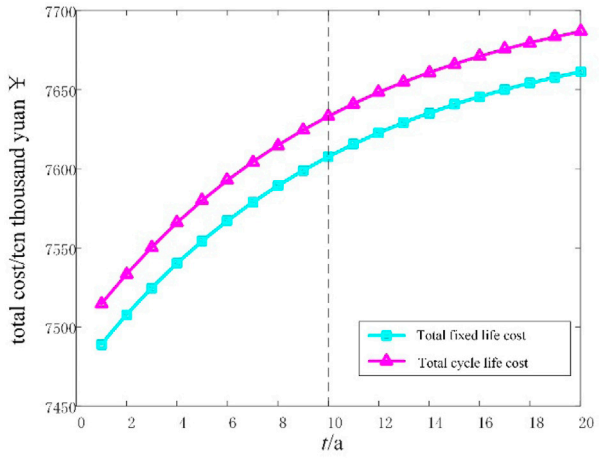

FIGURE 9
Total cost growth curve considering fixed and cycle life.

represented by IMF10. The decomposition results are shown in Figure 4. According to Eqs 8, 9, the maximum power volatility of 1 min or 10 min is calculated, and according to Eq. 10, the filtering order of the space-time filter $k = 4$ is selected when the volatility meets the requirements of grid connection.

It can be seen from Figure 3 that the wind-power grid-connected curve after leveling can well track the original wind-power curve. On the premise of meeting the grid-connected requirements, the smoothing effect is good and the fluctuation amplitude is small, which is reflected in the obvious change at the peak.

Figure 4 shows that the original wind power is decomposed by EEMD to obtain IMF components and aftereffect component, among which IMF8 and IMF9 are omitted and not drawn. As can be seen from the decomposed figure row, the high-frequency IMF1–IMF4 components fluctuate rapidly, but the fluctuation amplitude is small, and the variation range is −5 to 5 MW. The variation of IMF5–IMF10 components in the low-frequency part is relatively gentle, and the variation of the IMF10 component is the most gentle, but the fluctuation amplitude gradually increases. Therefore, the high-frequency part is suppressed by the hybrid energy storage system, and the low-frequency part enters the grid as the grid-connected power for load use.

6.2 Decomposition and reconstruction of hybrid energy storage

After EMD, the hybrid energy storage power $P_{\mathrm{HESS}}(t)$ obtained by the method in this paper is decomposed into seven IMF components and one aftereffect component from high to low according to the frequency range, and the aftereffect is represented by RS8, as shown in Figure 5.

The components decomposed by EMD are analyzed based on the grey correlation degree. Figure 6 shows the similarity analysis of each component of IMF and the residual component using the grey correlation degree analysis method. The results show that the components with similar correlation degrees in the comparison sequence are IMF1, IMF2, and IMF3, and the correlation degree is all greater than 0.4. In the other group, IMF4, IMF5, IMF6, IMF7, and RS8 had similar correlation degrees, and the correlation degrees were all less than 0.3. Therefore, the high-frequency part is composed of IMF1 + IMF2 + IMF3, and the low-frequency part is composed of the sum of IMF4–RS8 components, and the reconstructed power is allocated to the supercapacitor and lithium battery, respectively.

According to Figure 7, the supercapacitor bears the smooth output of the high-frequency part, and the charging and discharging times of the high-frequency part are frequent. The lithium battery undertakes the smooth output of the low-frequency part, and the low-frequency part charges and discharges gently, which is conducive to prolonging the service life of the lithium battery. The amount of power that needs to be suppressed is exactly in line with the technical characteristics of the two energy storage components.

Figure 8, for supercapacitor power distribution, with histogram representing the supercapacitor in the power of a typical day number distribution, blue curve representing power distribution fitting, and fitting curves representing the supercapacitor at 0 MW with normal symmetric distribution on both sides, shows that the supercapacitor in the calm wind power can complete charge and discharge of normal function.

6.3 Comparison and analysis of different methods

Supercapacitors and lithium batteries have their own characteristics and advantages and are widely used in engineering. Therefore, combining the advantages and complementary characteristics of the two types of energy storage, this paper adopts two different configuration schemes for comparative analysis. Scheme 1 uses the lithium battery as a single energy storage scheme; Scheme 2 adopts a hybrid energy storage scheme composed of lithium batteries and supercapacitors. According to different decomposition methods, the rated power and rated capacity under different schemes are configured. Assuming that the full life cycle of energy storage is 20 years, the investment cost of HESS under the two configuration schemes can be calculated according to the aforementioned methods. The specific calculation results are shown in Table 1.

According to the analysis in Table 1, except that the rated capacity of the supercapacitor determined by the EEMD method in Scheme 2 is lower than that determined by the proposed method, the rated power and rated capacity determined by the

proposed method are significantly lower than those configured by the EMD method and the EEMD method. In terms of the cost of configuration results, the EMD method has the highest cost, followed by the EEMD method. The economy of the proposed method is far better than that of the other methods, and the economy of the hybrid energy storage scheme is also far better than that of the single energy storage scheme. Hybrid energy storage system can utilize the advantages of two kinds of energy storage to reasonably configure the energy storage capacity and can reduce the system cost to the greatest extent under the premise of meeting the requirements of grid connection. It can be analyzed from Table 1 that the life cycle cost of the hybrid energy storage system decreases by 10% compared with that of the single energy storage system using the method in this paper.

6.4 Total cost analysis considering fixed life and cycle life

The fixed life setting of the energy storage battery is usually based on engineering experience. In this paper, the fixed life is 10.5 a. The cycle life calculated in this paper is 5.6 a. The growth curves of the total cost of fixed life and total cost of cycle life in the whole life cycle are shown in Figure 9. When the planning period is 10 A, the total cost of fixed life is 76, 074, 800 ¥, while the total cost of cycle life is 763, 30, 300 ¥, which decreases by 255,500 ¥ compared with the total cost of cycle life. Therefore, it is easy to reduce the investment amount by using the fixed life model to carry out the optimal allocation of hybrid energy storage. As the type of calculation cost increases, the gap between the total cost considering fixed life and the total cost considering cycle life becomes larger. If the total cost is calculated on a fixed lifetime basis, investors will be able to reduce the allocation of hybrid energy storage, resulting in excessive charging and discharging of existing energy storage equipment. Not only will the life of energy storage devices be reduced, but also the replacement of energy storage devices will be accelerated. Instead, the total cost of hybrid energy storage tends to increase. Therefore, it is not economical to calculate the total cost using the fixed-life model.

7 Conclusion

Aiming at the economic problem of capacity allocation in the hybrid energy storage system and the impact of battery energy storage life decay on system cost, this paper proposes a capacity optimal allocation model for the wind farm hybrid energy storage system based on the combined application of EEMD and EMD. Through the analysis of the example, the following conclusions are drawn:

1) Based on the power decomposition method combined with EEMD and EMD, the complementary characteristics between supercapacitors and lithium batteries are realized. The numerical example results show that the proposed method has better configuration effect than the traditional method using EEMD and EMD alone. The configuration capacity of lithium batteries and supercapacitors is reduced, which indirectly prolongs the service life of lithium batteries. The economy of system operation has been improved.
2) The frequency distribution rate is determined based on the grey correlation degree, so as to reconstruct the hybrid energy storage power. The high-frequency component is smoothly produced by the supercapacitor, and the low-frequency component is smoothly produced by the lithium battery. Through the calculation method of rated power and rated capacity of the energy storage system, the optimal value is determined, and a better effect of high- and low- frequency power distribution is obtained.
3) By comparing the two energy storage configuration schemes, it is further verified that the hybrid energy storage system scheme has more advantages in technology and economy than the single energy storage scheme, which is worthy of promotion and application.
4) The cycle life model considering battery life loss has higher battery capacity allocation than the fixed battery life model, and its investment cost is also very high, which is easy to make investors expect too high return on investment.

Data availability statement

The original contributions presented in the study are included in the article/Supplementary Materials; further inquiries can be directed to the corresponding author.

Author contributions

JS contributed to the conception of the research and data simulation. SH helped in conceptualization and methodology. CL wrote part of the manuscript. SL and JW contributed to data management.

Funding

This study was supported by the 2020 Anhui University Natural Science Research Project, under grant number KJ2020A0827.

Conflict of interest

The authors declare that the research was conducted in the absence of any commercial or financial relationships that could be construed as a potential conflict of interest.

Publisher's note

References

Bitaraf, H., Rahman, S., and Pipattanasomporn, M. (2015). Sizing energy storage to mitigate wind power forecast error impacts by signal processing techniques. *IEEE Trans. Sustain. Energy* 6 (4), 1457–1465. doi:10.1109/tste.2015.2449076

Ding, M., Wu, J., and Zhang, J. J. (2019). Capacity optimization method of hybrid energy storage system for wind power smoothing. *Acta Energiae Solaris Sin.* 40 (3), 593–599.doi:10.1109/ICMA.2014.6886029

Fu, J., Chen, J., Teng, Y., Deng, H., and Sun, Z. (2019). Energy management coordination control strategy for wind power hybrid energy storage system based on EEMD. *Trans. China Electrotech. Soc.* 34 (10), 2038–2046. doi:10.19595/j.cnki.1000-6753.tces.181729

Gan, W., Guo, J., Xiaomeng, A. I., Yao, W., Yang, B., Yao, L., et al. (2019). Multi-scale multi-index sizing of energy storage applied to fluctuation mitigation of wind farm. *Automation Electr. Power Syst.* 43 (09), 92–99. doi:10.7500/AEPS20180815002

Ge, L., Yuan, X. D., Wang, L., Lu, W., and Hu, B. (2017). Capacity configuration of hybrid energy storage system for distribution network optimal operation. *Power Syst. Technol.* 41 (11), 3506–3513. doi:10.13335/j.1000-3673.pst.2017.0479

Guo, L. J., Wei, B., Han, X. Q., and Li, W. (2020). Capacity optimal configuration of hybrid energy storage in hybrid AC/DC micro-grid based on ensemble empirical mode decomposition. *High. Volt. Eng.* 46 (2), 527–537. doi:10.13336/j.1003-6520.hve.20200131017

Guo, M., Mu, Y., Jia, H., Deng, Y., Xu, X., and Yu, X. (2021). Electric/thermal hybrid energy storage planning for park-level integrated energy systems with second-life battery utilization. *Adv. Appl. Energy* 4, 100064. doi:10.1016/j.adapen.2021.100064

Guo, T., Liu, Y., Zhao, J., Zhu, Y., and Liu, J. (2020). A dynamic wavelet-based robust wind power smoothing approach using hybrid energy storage system. *Int. J. Electr. Power & Energy Syst.* 116, 105579. doi:10.1016/j.ijepes.2019.105579

Han, X., Liang, Y., Ai, Y., and Li, J. (2018). Economic evaluation of a PV combined energy storage charging station based on cost estimation of second-use batteries. *Energy* 165, 326–339. doi:10.1016/j.energy.2018.09.022

Han, X., Tian, C. G., and Cheng, C. (2014). Power allocation method of hybrid energy storage system based on empirical mode decomposition. *Acta Energiae Solaris Sin.* 35 (10), 1889–1896. doi:10.3969/j.issn.0254-0096.2014.10.011

Han, X., Yu, X., Liang, Y., Li, J., and Zhao, Z. (2018). A game theory based coordination and optimization control methodology for a wind power generation hybrid energy storage system. *Asian J. Control* 20 (1), 86–103. doi:10.1002/asjc.1518

Han, X., Zhao, Z., Li, J., and Ji, T. (2017). Economic evaluation for wind power generation–hybrid energy storage system based on game theory. *Int. J. Energy Res.* 41 (1), 49–62. doi:10.1002/er.3591

He, J., Shi, C., Ma, M., Huo, Q., Xin, K., and Wei, T. (2020). Bi-level optimal configuration method of hybrid energy storage system based on meta model optimization algorithm. *Electr. Power Autom. Equip.* 40 (7), 157–167. doi:10.16081/j.epae.202007001

Hemmati, R., Saboori, H., and Siano, P. (2017). Coordinated short-term scheduling and long-term expansion planning in microgrids incorporating renewable energy resources and energy storage systems. *Energy* 134, 699–708. doi:10.1016/j.energy.2017.06.081

Li, S., Pischinger, S., He, C., Liang, L., and Stapelbroek, M. (2018). A comparative study of model-based capacity estimation algorithms in dual estimation frameworks for lithium-ion batteries under an accelerated aging test. *Appl. energy* 212, 1522–1536. doi:10.1016/j.apenergy.2018.01.008

Li, X., Ma, R., Wang, S., Zhang, Y., Li, B., and Fang, C. (2020). Operation control strategy for energy storage station after considering battery life in commercial park. *High. Volt. Eng.* 46, 62–70. doi:10.13336/j.1003-6520.hve.20191227007

Lin, R., Ren, J., Liu, Y., Lee, C. K., Ji, P., Zhang, L., et al. (2021). Sustainability prioritization of energy systems under hybrid information and missing information based on the improved grey relational analysis. *Sustain. Energy Technol. Assessments* 47, 101543. doi:10.1016/j.seta.2021.101543

Lou, S., Yaowu, W. U., Cui, Y., Lin, Y. I., Wang, J., and Hou, T. (2014). Operation strategy of battery energy storage system for smoothing short-term wind power fluctuation. *Automation Electr. Power Syst.* 38 (2), 17–22+58. doi:10.7500/AEPS201212049

Mamun, A. A., Liu, Z., Rizzo, D. M., and Onori, S. (2018). An integrated design and control optimization framework for hybrid military vehicle using lithium-ion battery and supercapacitor as energy storage devices. *IEEE Trans. Transp. Electrific.* 5 (1), 239–251. doi:10.1109/TTE.2018.2869038

Sami, S. S., Cheng, M., Wu, J., and Jenkins, N. (2018). A virtual energy storage system for voltage control of distribution networks. *CSEE J. Power Energy Syst.* 4 (2), 146–154. doi:10.17775/CSEEJPES.2016.01330

Sun, Y., Zhao, Z., Yang, M., Jia, D., Pei, W., and Xu, B. (2019). Research overview of energy storage in renewable energy power fluctuation mitigation. CSEE J. *Power Energy Syst.* 6, 160–173. doi:10.17775/CSEEJPES.2019.01950

Tabart, Q., Vechiu, I., Etxeberria, A., and Bacha, S. (2017). Hybrid energy storage system microgrids integration for power quality improvement using four-leg three-level NPC inverter and second-order sliding mode control. *IEEE Trans. Ind. Electron.* 65 (1), 424–435. doi:10.1109/tie.2017.2723863

Wang, Y., Wu, M. K., Zhou, Z., and Ma, H. (2017). Quantitative analysis model of power load influencing factors based on improved grey relational degree. *Power Syst. Technol.* 41 (06), 1772–1778. doi:10.13335/j.1000-3673.pst.2016.1852

Yuan, Y., Sun, C., Li, M., and Li, Q. (2015). Determination of optimal supercapacitor-lead-acid battery energy storage capacity for smoothing wind power using empirical mode decomposition and neural network. *Electr. Power Syst. Res.* 127, 323–331. doi:10.1016/j.epsr.2015.06.015

Zhang, Q., Li, X., Yang, M., Cao, Y., and Li, P. (2016). Capacity determination of hybrid energy storage system for smoothing wind power fluctuations with maximum net benefit. *Trans. China Electrotech. Soc.* 31 (14), 40–48. doi:10.19595/j.cnki.1000-6753.tces.2016.14.005

Zheng, H., Xie, L. R., Ye, L., Lu, P., and Wang, K. F. (2021). Hybrid energy storage smoothing output fluctuation strategy considering photovoltaic dual evaluation indicators. *Trans. china Electrotech. Soc.* 36 (09), 1805–1817. doi:10.19595/j.cnki.1000-6753.tces.201058

Zheng, J., Cheng, J., and Yang, Y. (2013). Modified EEMD algorithm and its applications. *Jouranl Vib. Shock* 32 (21), 21–46. doi:10.13465/j.cnki.jvs.2013.21.007